Tellus (1991), *43B*, 156–170

Latitudinal distribution of sources and sinks of CO_2: results of an inversion study

By I. G. ENTING and J. V. MANSBRIDGE*, *CSIRO, Division of Atmospheric Research, Private Bag 1, Mordialloc, Victoria 3195, Australia*

(Manuscript received 14 May 1990; in final form 25 September 1990)

ABSTRACT

A two-dimensional inversion calculation is used to estimate the distribution of surface sources of atmospheric CO_2 in space and time. These estimates are then modified to account for the role of CO and CH_4 in the atmospheric carbon budget. The results confirm previous estimates of a weak (oceanic) sink in the southern hemisphere of 1.3 Gt C yr^{-1} and a northern sink of 1.9 Gt C yr^{-1}. These sink strengths are disproportionate to the ocean areas although, compared to our previous studies, the CO correction has reduced the degree of disproportion. Because of a number of near cancellations, the CO correction leads to little change in the net carbon budget of the tropics. Combining the net release estimate for the region 12° S to 12° N with independent estimates of oceanic CO_2 release implies that, in this region, the terrestrial biomass is nearly constant or even slowly increasing, in spite of massive deforestation. The implications for the global carbon budget are discussed.

1. Introduction

The extent to which the terrestrial biota contribute to long-term changes in atmospheric CO_2 concentrations has long been a contentious question in carbon cycle studies. Various workers have made strong suggestions of a net source due to forest clearing and a net sink due to regrowth and/or biotic fertilisation due to increasing CO_2 concentrations (e.g., Houghton et al., 1983; Olson, 1982). There have been corresponding attempts to modify ocean models to account for the uptake of excess CO_2 from deforestation (e.g. Siegenthaler, 1983). A recent study by Tans et al. (1990) has increased the contentiousness of the issue by suggesting the northern hemisphere oceans are taking up very little of the fossil carbon released into the atmosphere and further, that the southern oceans are also unlikely to be taking up a large amount of carbon.

Four main approaches have been used in the past to estimate the biotic contribution to atmospheric CO_2 levels.

(i) Direct estimates of biotic releases (e.g. Houghton et al., 1983);

(ii) Interpretation of global scale budgets (e.g., Siegenthaler and Oeschger, 1987);

(iii) Determination of spatial distribution of sources (e.g. Enting and Mansbridge, 1989, Tans et al. 1989);

(iv) Interpretation of changes in $\delta^{13}C$ (e.g. Siegenthaler and Oeschger, 1987).

The present study looks at the 2nd and 3rd of these approaches, i.e., those that involve the interpretation of atmospheric CO_2 data. Most attention is given to the approach of determining the spatial distribution of the sources so that the source regions can be used to help identify the source/sink processes. This study is a refinement of our earlier inversion studies (Enting and Mansbridge, 1989). We have made a number of small changes to our transport model and the fields that define the transport. We have also considered the role of CO in the atmospheric carbon budget. Although the amounts of carbon transported as CO are large enough to be comparable

* Present address: CSIRO, Division of Oceanography Marine Laboratories, GPO Box 1538, Hobart, Tas 7001, Australia.

to regional carbon exchanges from CO_2, a more detailed analysis shows that the CO budget involves a number of near cancellations that make its net effect on the atmospheric carbon budget relatively small, even on a regional basis.

2. Data

The main thrust of the present study is the inversion of the space-time variation of surface concentrations of CO_2. Table 1 lists the sites for which we use data. As in our previous study, we aim to consider an average year, rather than attempting to follow the interannual variation as was done by Tans et al. (1989). We represent the temporal variation by a linear trend of 1.5 ppmv per year for all sites plus a spatially varying seasonal cycle consisting of sinusoids of periods 1 year and 6 months. The spatial variations of these components and of the mean interhemispheric gradient, which we take as fixed, are represented by splines. This approach was used by Tans et al. (1989) in contrast to the spectral representation of spatial variation used in our previous study (Enting and Mansbridge, 1989). The spline fitting was performed in sin(latitude) coordinates. The stiffness of the spline was chosen so as to give 50% attenuation to variations whose wavelength was $\Delta\sin(\text{latitude}) = 1$.

Table 1. *Sites for which CO_2 data (primarily from Conway et al., 1988; Beardsmore and Pearman, 1987; Tans et al., 1990) were used in the inversion*

Code	Site	Latitude	Usage
AMS	Amsterdam Is.	38S	mean
ASC	Ascension Is.	8S	both
AVI	Virgin Is.	18N	both
AZR	Azores	39N	both
BRW	Point Barrow	71N	both
CBA	Cold Bay	55N	both
CGO	Cape Grim, Tasmania	41S	both*
CHR	Christmas Is.	2N	mean
GMI	Guam	13N	both
HBA	Halley Bay	76S	both
KEY	Key Biscayne	26N	both
KUM	Cape Kumakahi	20N	both
MAW	Mawson, Antarctica	68S	cycle
MBC	Mould Bay	76N	cycle
MID	Midway Is.	28N	mean
MQI	Macquarie Is.	54S	cycle
NWT	Niwot Ridge	40N	cycle
PSA	Palmer Station	65S	both
SEY	Seychelles	5S	both
SHM	Shemya Is.	53N	mean
SMO	Samoa	14S	both
SPO	South Pole	90S	both
STM	Ocean Station "M"	66N	both

Codes are as used in the original references. Usage is "mean" if only annual mean is used, "cycle" if only annual cycle is used and "both" if both mean and cycle are used.* For Cape Grim, the seasonal cycle is taken from CSIRO data while annual mean is taken from the GMCC data (Tans et al., 1990) to ensure intercomparability.

Compared to spectral methods, splines give a more localised fit, acting as a type of digital filter so that the fit in the southern hemisphere is much less influenced by the form of the fit in the northern hemisphere than is the case when spectral coefficients are fitted by regression analysis. This difference is of little significance in the present study but it may be important in our on-going studies of Southern Ocean sources (see Pearman and Hyson, 1986; Francey et al., 1988).

For each spline fit, the data is weighted by its standard deviation. The interhemispheric gradient is treated somewhat differently from the seasonal cycle and a different data set is used as indicated in Table 1. The interhemispheric gradient is fitted to the NOAA/GMCC data from Tans et al. (1990)

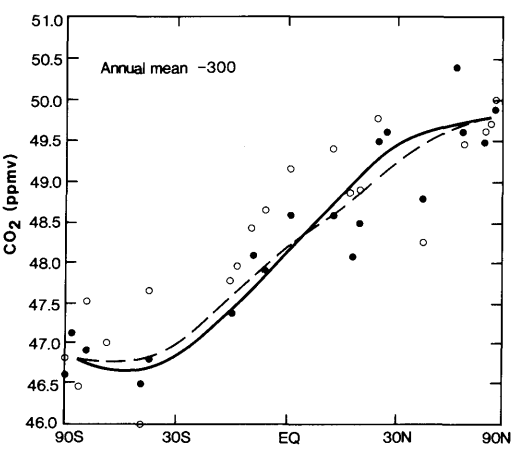

Fig. 1. Smoothing spline fits to the interhemispheric gradient and the data points used in constructing the fit (solid circles). Open circles are the data analysed by Pearman and Hyson (1986) with a constant concentration added so as to simplify the comparison. Solid curve is spline with data points weighted by individual standard deviations, dashed curve fitted with each point having equal weight.

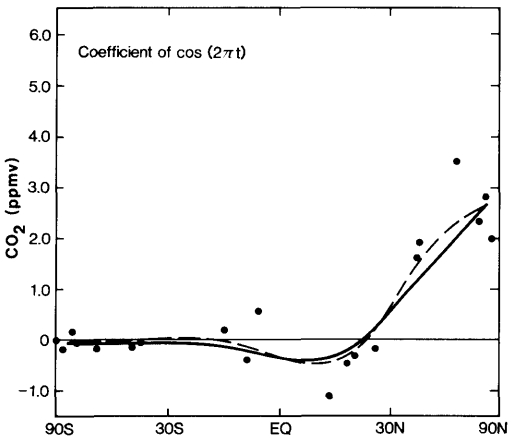

Fig. 2. Smoothing spline fits to the coefficient of $\cos(2\pi t)$ and the data points used in constructing the fits (as for Fig. 1).

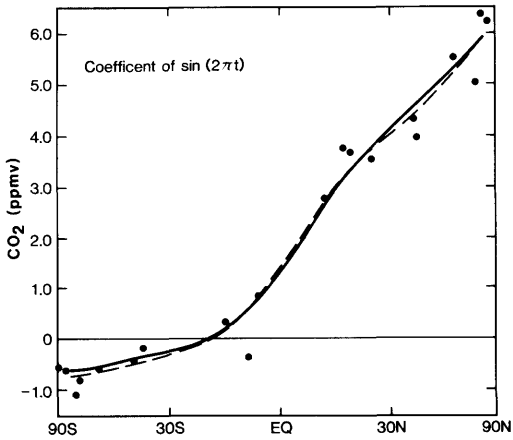

Fig. 3. Smoothing spline fits to the coefficient of $\sin(2\pi t)$ and the data points used in constructing the fits (as for Fig. 1).

(with Niwot Ridge being excluded because it is a high altitude site). For each site, α, they present an average concentration $x_{0\alpha}$ corrected to give an equivalent mid-1987 mean value. The standard deviation used in weighting the splines is obtained from the variance of the individual values. The seasonal cycle is constructed by regression analysis of monthly mean NOAA/GMCC data given by Conway et al. (1988) supplemented by records from Cape Grim (1976–1984), Macquarie Island (1980–1987) and Mawson, Antarctica (1985–1988). These data were obtained from Beardsmore and Pearman (1987) as updated by D. J. Beardsmore (personal communication).

Table 2. *Coefficients defining time variation of surface CO_2 concentration for each zone; the model uses 20 equal area zones; latitudes are tabulated to the nearest degree*

Zone	Latitudes	1	$\cos(2\pi t)$	$\sin(2\pi t)$	$\cos(4\pi t)$	$\sin(4\pi t)$
1	90S –64S	46.78	−0.07	−0.63	−0.01	−0.09
2	64S –53S	46.70	−0.08	−0.58	−0.03	−0.06
3	53S –44S	46.64	−0.08	−0.49	−0.03	0.00
4	44S –37S	46.65	−0.06	−0.39	−0.02	−0.07
5	37S –30S	46.74	−0.05	−0.29	−0.02	0.14
6	30S –24S	46.91	−0.04	−0.19	−0.02	0.20
7	24S –18S	47.14	−0.06	−0.05	−0.02	0.24
8	18S –12S	47.40	−0.11	0.16	−0.03	0.23
9	12S – 6S	47.67	−0.20	0.47	0.04	0.18
10	6S –Eq	47.95	−0.31	0.94	0.11	0.07
11	Eq– 6N	48.22	−0.39	1.51	0.20	−0.08
12	6N–12N	48.47	−0.41	2.14	0.29	−0.29
13	12N–18N	48.74	−0.32	2.77	0.36	−0.52
14	18N–24N	49.03	−0.08	3.32	0.39	−0.77
15	24N–30N	49.30	0.29	3.78	0.41	−1.04
16	30N–37N	49.47	0.77	4.19	0.41	−1.33
17	37N–44N	49.57	1.27	4.59	0.43	−1.63
18	44N–53N	49.65	1.75	5.01	0.51	−1.94
19	53N–64N	49.71	2.20	5.44	0.63	−2.26
20	64N–90N	49.77	2.62	5.88	0.79	−2.56

For each site, α, the CO_2 concentrations were fitted in a least squares manner by a function of the form

$$c_\alpha(t) = c_\alpha + p_\alpha t + x_{1\alpha}\cos(2\pi t) + x_{2\alpha}\sin(2\pi t) + x_{3\alpha}\cos(4\pi t) + x_{4\alpha}\sin(4\pi t). \quad (1)$$

A quadratic term, $q_\alpha t^2$, was included in the analysis of the longer records from Cape Grim and Macquarie Island. The standard deviations of the regression estimates of each of the coefficients $x_{j\alpha}$, $j = 1$ to 4 were used as weights in the spline fit of the seasonal coefficients.

For each $j = 0$ to 4 we fitted a smoothing spline to the coefficients, $x_{j\alpha}$, weighted as described above. Figs. 1, 2 and 3 show the coefficients $x_{j\alpha}$, plotted as solid circles, and the spline fit (solid curve) for $j = 0$, 1, 2, respectively. For comparison, the spline fits with equal weighting of each point are shown as the dashed curves in each case. In Fig. 1 we also show, as open circles, the concentration data analysed by Pearman and Hyson (1986), with a constant concentration added so as to overlap the more recent data. (This shift was chosen so that our spline fit matched the Pearman and Hyson polynomial fit at the South Pole.) The differences are discussed in Section 5 below. For use in the inversion calculation we take the values of the spline fits, $\bar{x}_{jk}$, at the mid-points of each of our zones ($k = 1$ to 20) and construct a set of functions $\bar{c}_k$ specified by

$$\bar{c}_k(t) = c_0 + 1.5t + \bar{x}_{0k} + \bar{x}_{1k}\cos(2\pi t) + \bar{x}_{2k}\sin(2\pi t) + \bar{x}_{3k}\cos(4\pi t) + \bar{x}_{4k}\sin(4\pi t). \quad (2)$$

The coefficients $\bar{x}_{jk}$ are listed in Table 2.

3. Two-dimensional modelling

3.1. Transport model

The inversion of the distribution of CO_2 is performed using a two-dimensional numerical model of atmospheric transport. The basic model was described by Enting and Mansbridge (1986) and some preliminary studies were reported by Enting and Mansbridge (1987a). The model was used for estimating surface sources of CO_2 by Enting and Mansbridge (1989) and some sensitivity studies are reported by Mansbridge and Enting (1989). The model represents atmospheric transport by a combination of advection and eddy diffusion. The most notable characteristic of our modelling is the use of transport coefficients derived from the transport characteristics of a three-dimensional general circulation model by Plumb and Mahlman (1987). The model has undergone three main changes since our earlier study (Enting and Mansbridge, 1989).

(i) We have modified the transport coefficients.

(ii) We have changed the way in which the lower boundary is treated, thus refining the relation between surface sources and surface concentrations.

(iii) We have included an additonal source of CO_2 due to the oxidation of CO in the free atmosphere. This is described in more detail in the following subsection.

We now describe these changes in more detail (see also Mansbridge and Enting, 1989).

The first change in our transport fields is that we now use values that are linearly interpolated in space and time from the coefficients calculated by Plumb and Mahlman. We found that our previous use of a spectral representation tended to over-smooth the coefficients, especially at the tropopause. Secondly we have modified the coefficients so as to effectively lower the model tropopause. The coefficients calculated by Plumb and Mahlman had, as an artifact of their computational procedure, an unrealistically high tropopause (R. A. Plumb, personal communication). This was modified by re-interpreting the levels at which Plumb and Mahlman had calculated their coefficients; their 150 mb level was re-interpreted as 250 mb and levels above and below this were re-scaled in a linear manner such that the correction went to zero at the boundaries. We then enhanced the vertical diffusion in the lowest layers, multiplying K_{pp} by a factor which was 3 at 950 mb and decreased linearly to 1 at 750 mb. This change was made on the basis of studies which showed that the seasonal cycle of CO_2 (as compared to data from Tanaka et al., 1987; Friedli et al., 1987 and Bolin and Bischof, 1970) was attenuated much too rapidly when using the original fields from Plumb and Mahlman (see also Enting and Mansbridge, 1987a). The possibility of using the height dependence of the seasonal cycle of CO_2 to help calibrate model

transport was also noted by Tans et al., 1989. In contrast, Pearman and Hyson (1986) calibrated their vertical transport using CCl_3F data and used the vertical attenuation of the CO_2 cycle to validate this calibration.

The vertical and horizontal resolution of the model can be changed, subject to the available computing power and the need to reduce the time step so as to ensure numerical stability when the resolution is increased. The runs performed for this study used 20 equal area zones and 20 equal pressure levels. We apply lower bounds to the diffusion coefficients in a slightly different way to our earlier calculations. The horizontal diffusion has a lower bound $K_{yy} \leqslant 10^4 \cos^2(\text{latitude})$. The vertical diffusion has a lower bound of $K_{zz} \leqslant 1\ \text{m}^2\ \text{s}^{-1}$ in the troposphere and $K_{zz} \leqslant 0.1\ \text{m}^2\ \text{s}^{-1}$ in the stratosphere. (For use in the model these bounds are re-expressed in terms of K_{pp}.)

In earlier studies with our model, we specified the surface concentration by equating it to the concentration in the lowest layer. The inverse calculation of determining surface sources was performed by forcing the lowest layer to follow a specified concentration history. The surface source was then determined from mass-balance in the lowest layer. (Essentially the same procedure was used by Tans et al., 1989). This procedure is only accurate to first order in the grid spacing while all other aspects of our transport model are accurate to second order in the grid spacing. This is a matter of concern since the study by Newsam and Enting (1988) suggests that the treatment of the surface will be one of the more sensitive aspects of the inverse problem of deducing surface sources from surface concentrations.

In the present version of the model, we assume that the surface concentration and the concentrations in the lowest two layers are connected by a quadratic function of pressure. The surface source is taken as

$$s(x) = K_{pp} \frac{\partial c}{\partial p}. \tag{3}$$

For forward calculations, we introduce a specified source into the lowest layer and integrate the model equations. The surface concentration is calculated (if required) by fitting the quadratic function to the two calculated concentrations for the lowest layers and the gradient at the surface as determined from eq. (3). The inverse calculation proceeds by taking the calculated concentrations from the lowest two layers and combining these with the specified surface concentration to fit the parabolic profile. The surface source is then determined from the gradient of this parabola. This source is then used as input to the lowest layer as the model is integrated. Mansbridge and Enting (1989) present a range of sensitivity studies comparing several approaches to treating this surface boundary condition in an idealized model.

Our new approach to treating the surface requires a value for K_{pp} at the surface. In the model this would represent transport within a zonally-averaged boundary layer; there is little basis for choosing a value for this parameter. The coefficients defined by Plumb and Mahlman (1987) arise from large scale eddy motions and so go to zero at the surface, and in any case we have found it necessary to modify their coefficients near the surface. We have chosen the surface coefficient to correspond to $10\ \text{m}^2\ \text{s}^{-1}$ as a somewhat arbitrary number of similar size to the transport coefficients in the free atmosphere. Fortunately the deduced sources are only moderately sensitive to the value of this parameter. Reducing it to $1\ \text{m}^2\ \text{s}^{-1}$ only reduces the estimated source strengths by 50% or less due to compensating changes in the vertical profiles.

The other aspect of our inverse calculation that we have changed is that we only invert the surface concentrations for zones 2 to 20. For zone 1 (90°S to 64°S), we specify the source to be zero rather than specifying the concentration. This is done to reflect the absence of sources on the Antarctic continent. Compared to the procedure of inverting the concentrations for all zones, the changes are very small except for zone 2 and of course zone 1. The details are of little concern in the present study and will be discussed in subsequent studies of Southern Ocean sources.

The primary validation of the transport used in our model is, of course, the original GCM from which the coefficients are derived and in particular its ability to produce a reasonable atmospheric heat budget. Since the main mechanism of the transport across the tropics is the seasonal movement of the ITCZ which leads to alternating seasonal mixing into each hemisphere, the validity of the transport of heat from the tropics is an

important part of the validation of interhemispheric transport.

For the purpose of validating the transport coefficients using dynamically inactive tracers, ^{85}Kr provides one of the most suitable tests when modelling a constituent such as CO_2 which has an atmospheric lifetime of many years. The distribution of CCl_3F is rather harder to use because it is sensitive to the accuracy with which the stratospheric sink and the transport across the tropopause are modelled. We have simulated the distribution of ^{85}Kr, tuning the source strength to match the atmospheric concentration and then comparing the interhemispheric gradient to the data of Weiss et al. (1983). As might be expected from our discussion of the heat budget in the GCM, we obtained our best fit *before* we tuned the vertical transport to fit the observed seasonality of CO_2 in the upper troposphere. Adjustments to climatically consistent transport fields will not normally preserve such consistency. Our tuning of the vertical transport led to a slightly reduced interhemispheric gradient of ^{85}Kr. A full re-calibration of the atmospheric transport is a severely underdetermined problem and it would in any case obviate the advantages of basing the transport on a GCM. Without further indications of the extent to which the ^{85}Kr data are zonally representative it therefore seem premature to make further modifications to the transport in order to improve the fit. If the ^{85}Kr are zonally representative, then it is probable that our inversions over-estimate the north-south gradient of the source strengths.

3.2. *CO source model*

The potential importance of CO in determining atmospheric CO_2 sources was noted by Enting and Mansbridge (1989). We pointed out that inverse problems can be very sensitive to errors in the model assumptions and that our inverse calculations assumed solely surface sources when in fact there was a significant source in the free atmosphere. Newsam and Enting (1988) had previously noted the distinct differences in the relation between sources and surface concentrations for surface sources as opposed to vertically-averaged sources. A more complete analysis of inverse problems involving sources in the free atmosphere is given by Enting and Newsam (1990a). Their results indicate that a source of CO_2 from CO oxidation (which is concentrated in the tropics) will appear as a more widely-spread apparent surface source if the surface data is inverted by the method used in our previous modelling study.

In our discussion of CO budgets, we shall use units of gigatonnes of *carbon* (Gt C) in the various species, rather than the masses of the total of all elements in each species. Crutzen and Gidel (1983, see also Crutzen, 1987) performed a modelling study and estimated the global CO source as 1.15 Gt C (2.69 Gt CO), comprising 0.28 Gt C from industrial sources, 0.24 Gt C from oxidation of CH_4 and 0.63 Gt C of other (mainly biotic) sources. These were balanced by sinks of 0.88 Gt C from oxidation by OH and 0.27 Gt C from destruction of CO at the surface of the earth. They also estimated the spatial distribution of these various sources. Seiler and Conrad (1987) produced an alternative set of estimates. They split the "other" sources into biomass burning (0.43 Gt C), oxidation of non-methane-hydrocarbons (0.39 Gt C) and smaller contributions from direct emissions from vegetation and oceans. Seiler and Conrad estimated that sources exceeded sinks by 32%, implying a growth in atmospheric CO. The observational situation is unclear, with CO increases being observed in the northern hemisphere but not in the southern hemisphere. Fraser et al., (1986) reported further modelling studies of CO using estimated sources totalling 1.2 Gt C (2.8 Gt CO), but found some difficulty in reproducing observed concentrations.

For the present study, we use a set of compromise values for CO sources and sinks. Table 3 shows the various contributions, including estimates of the ultimate source of the CH_4 that is oxidised to CO. We assume that only half the methane production goes to CO, the rest being oxidised to soluble organics which are deposited in the source region. The annual total CO source is 1.03 Gt C (2.4 Gt CO). The direct "biotic" sources include both actual CO emissions and emissions of short-lived organic species that are rapidly oxidised to CO; we set these sources to 0.56 Gt C. The fossil CO source was taken to be 0.26 Gt C. The sources from CH_4 total 0.21 Gt C (0.5 Gt CO produced); these are divided into 0.04 Gt C fossil and 0.17 Gt C biotic. We further divided this source into wetland sources of 0.05 Gt C and 0.12 Gt C of other sources. This division is of little importance in the present study but could be important in future studies of isotopic variation

Tellus B/43/2-6

Table 3. *Distribution of non-CO_2 sources and sinks of atmospheric carbon*

Zone	oxidation (sink)	Soils (sink)	Fossil $CO + CH_4$	Biotic CO	Wetland CH_4	Other CH_4
	r_{OH}	r_{SOIL}	r_{FOSSIL}	r_{BIOTA}	r_{WET}	r_{CH_4}
1	0.014	0.000	0.0000	0.000	0.000	0.000
2	0.017	0.000	0.0002	0.007	0.000	0.000
3	0.023	0.000	0.0015	0.013	0.000	0.002
4	0.031	0.000	0.0060	0.009	0.005	0.012
5	0.040	0.015	0.0119	0.009	0.011	0.016
6	0.047	0.022	0.0086	0.019	0.029	0.046
7	0.053	0.027	0.0067	0.030	0.030	0.037
8	0.060	0.030	0.0028	0.044	0.032	0.019
9	0.068	0.033	0.0067	0.063	0.038	0.074
10	0.073	0.035	0.0086	0.084	0.040	0.101
11	0.079	0.038	0.0093	0.106	0.039	0.129
12	0.081	0.042	0.0108	0.121	0.036	0.117
13	0.079	0.049	0.0138	0.131	0.028	0.090
14	0.076	0.069	0.0295	0.119	0.016	0.113
15	0.071	0.086	0.0373	0.107	0.013	0.125
16	0.062	0.097	0.1848	0.092	0.016	0.040
17	0.052	0.114	0.2036	0.044	0.039	0.030
18	0.039	0.142	0.2627	0.000	0.142	0.029
19	0.022	0.142	0.1849	0.000	0.324	0.020
20	0.013	0.057	0.0103	0.000	0.162	0.000
Total	0.86	0.17	0.30	0.56	0.05	0.12

CO sources include non-methane hydrocarbons and other species that are rapidly oxidised to CO. For each zone the proportion of each source for the zone is quoted. "Total" gives the source strength, in Gt C yr^{-1}, in our preferred atmospheric carbon budget.

since the two components differ significantly in both spatial distribution and isotopic composition. The 1.03 Gt C of CO sources are balanced by sinks of 0.86 Gt C (2.0 Gt CO) for oxidation by OH and 0.17 Gt C (0.4 Gt CO) destruction at the earth's surface.

For the purpose of the budget analysis presented in the following section, we need the spatial distribution of the sources. The only aspect of the CO budget used directly in the model runs is the distribution of the CO_2 source from oxidation of CO in the free troposphere. We assume, as a first approximation, a seasonally invariant source that is vertically uniform throughout the troposphere. The latitudinal distribution of this source is taken from Crutzen and Gidel (1983) and is shown in the "oxidation" column of Table 3. These proportions are multiplied by the total (0.86 Gt C yr^{-1}) and then, for each zone, are distributed uniformly through the troposphere as a CO_2 source in the model runs.

The distributions of the surface CO and CH_4 contributions are also taken from Crutzen and Gidel (1983) except for the contribution of CH_4 from wetlands which is taken from Matthews and Fung (1987). The relative proportions of the sources for each zone are shown in Table 3 (having been converted to our equal-area scale). This table also shows our proposed budget. These proportions are multiplied by the total source from CO and combined with the model results as described in the following section.

4. Results

The correction we apply to account for the role of CO can be best understood if we consider the

atmospheric budgets of CO_2, CO and CH_4 whose source components we denote X, Y and Z, respectively. We propose a CO_2 budget, typical of the period 1978–84 from which the CO_2 data were obtained, with a fossil carbon release of 5.2 Gt C yr^{-1}. The CO_2 component is:

$$\frac{\partial}{\partial t}[CO_2] = X_{\text{fossil}CO_2} + X_{CO+OH} + X_{CO+\text{soil}} + X_{\text{biota}} + X_{\text{ocean}}. \quad (4)$$

The amounts of carbon (Gt C yr^{-1}) in our proposed budget are:

$$3.19 = 4.90 + 0.86 + 0.17 - (2.74 - x) - x. \quad (5)$$

Our proposed CO budget, for which we assume no growth, is:

$$0 = Y_{\text{fossil}CO} + Y_{CH_4+OH} + Y_{\text{biota}} - X_{CO+OH} - X_{CO+\text{soil}} \quad (6)$$

The amounts of carbon (Gt C yr^{-1}) are taken as:

$$0 = 0.26 + 0.21 + 0.56 - 0.86 - 0.17. \quad (7)$$

For CH_4 we ignore the growth (which is less than 1% yr^{-1}) as being small relative to the 10% yr^{-1} turnover. Our proposed CH_4 contribution to the atmospheric carbon budget is (recalling that only half the methane production goes to CO):

$$0 = 0.5Z_{\text{fossil}} + 0.5Z_{\text{wetlands}} + 0.5Z_{\text{other}} - Y_{CH_4+OH} \quad (8)$$

The amounts of carbon (Gt C yr^{-1}) are taken as:

$$0 = 0.04 + 0.05 + 0.12 - 0.21. \quad (9)$$

The total atmospheric carbon budget is given by adding these budgets to give

$$\frac{\partial}{\partial t}[CO_2] = X_{\text{fossil}CO_2} + X_{\text{biota}} + X_{\text{ocean}} + Y_{\text{fossil}CO} + Y_{\text{biota}} + 0.5Z_{\text{fossil}} + 0.5Z_{\text{wetlands}} + 0.5Z_{\text{other}}. \quad (10)$$

The non-fossil sources are given by:

$$S_{\text{nonfossil}} = X_{\text{biota}} + X_{\text{ocean}} + Y_{\text{biota}} + 0.5Z_{\text{wetlands}} + 0.5Z_{\text{other}}. \quad (11)$$

The CO_2 inversion (with the "oxidation" source from CO included) gives an estimate of the surface CO_2 source:

$$S_{CO_2} = X_{\text{fossil}CO_2} + X_{CO+\text{soil}} + X_{\text{biota}} + X_{\text{ocean}}. \quad (12)$$

Thus the non-fossil carbon sources are obtained from

$$S_{\text{nonfossil}} = S_{CO_2} - X_{CO+\text{soil}} - X_{\text{fossil}CO_2} + Y_{\text{biotic}} + 0.5Z_{\text{wetlands}} + 0.5Z_{\text{other}}. \quad (13)$$

In terms of the information in Table 3, the non-fossil source distribution is given by

$$S_{\text{nonfossil}}(j) = S_{CO_2}(j) - 0.17r_{\text{SOIL}}(j) - 4.9r^*_{\text{FOSSIL}}(j) + 0.56r_{\text{BIOTA}}(j) + 0.05r_{\text{WET}}(j) + 0.12r_{CH_4}(j). \quad (14)$$

Our fossil fuel distribution $r_{\text{FOSSIL}}(j)$ as given in Table 3 has been smoothed using a 3-point filter with weights $\frac{1}{4}$, $\frac{1}{2}$, $\frac{1}{4}$ to produce $r^*_{\text{FOSSIL}}(j)$. This is for consistency with the model results which are smoothed sources because the model inverts smoothed concentrations. The other distributions are already smoothed functions derived from modelling, except for $r_{\text{WET}}(j)$ which makes only a very small contribution.

Fig. 4 shows the dominant contributions in-

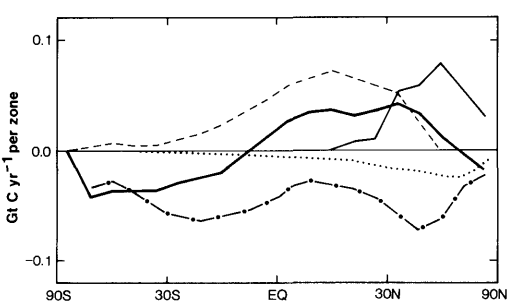

Fig. 4. Difference (bold continuous line) between the deduced carbon sources calculated with and without the inclusion CO in the model and the main contributions to this difference. Chain curve is lowering of estimated sources due to oxidation source in free atmosphere, dashes are biotic CO source and light continuous line, $0.3r^*_{\text{FOSSIL}}(j)$, represents 0.3 Gt C yr^{-1} adjustment to the fossil fuel source that is subtracted from the total CO_2 source. Dotted curve is CO sink (i.e., CO_2 source) in soils. Our fossil fuel distribution $r_{\text{FOSSIL}}(j)$ has been smoothed to give $r^*_{\text{FOSSIL}}(j)$ for consistency with the model results which are smoothed sources because the model inverts smoothed concentrations.

volved in converting a CO_2 budget into a carbon budget. It is seen that while individual processes are strong enough to be a significant fraction of the carbon budget on regional scales, the change to the surface carbon budget caused by including CO in the model (as shown as the bold continuous line) is relatively small. The chain curve shows the change in the calculated non-fossil surface CO_2 sources that result from including a source in the free atmosphere. This correction is more widely spread than the distribution of CO oxidation; this is in qualitative agreement with the analysis by Enting and Newsam (1990a). The extent to which this spread occurs in our numerical model is even greater than in the purely diffusive model considered by Enting and Newsam. This is because much of the CO oxidation is occuring in a region of upward transport and so the local influence of this CO_2 source is reduced from what would occur in a purely diffusive atmosphere. The dashes in Fig. 4 represent the biotic source of CO and the light continuous line represents the non-CO_2 fossil carbon release. This is the difference between subtracting a 4.9 Gt C yr^{-1} fossil CO_2 source as indicated by eq. (14) and subtracting a 5.2 Gt C yr^{-1} fossil carbon source as if all carbon was released as CO_2, i.e., assuming $S_{\text{nonfossil}}(j) \approx S_{CO_2}(j) - 5.2 r^{*}_{\text{FOSSIL}}(j)$. The dotted curve is the CO soil sink. These three main corrections combine with the other minor contributions to give a correction that is nearly uniform over the tropics and northern hemisphere. When they are combined with the change (chain curve) in the inverted souces the main consequence is an increase of southern hemisphere sinks by about 0.25 Gt C yr^{-1} with a corresponding decrease in northern hemisphere sinks. In terms of conventional interpretations of oceanic uptake of CO_2, this represents a small correction. However Tans et al. (1990) propose total ocean uptake in the range 0.5 to 1.0 Gt C yr^{-1}, in which case the CO correction becomes quite important. The disparity between north and south, as shown in Fig. 5, is less than in our earlier study.

Fig. 5 shows the estimated annual mean non-fossil surface carbon source as a function of latitude, calculated as described above. The general features are the same as in our earlier study (Enting and Mansbridge, 1989) and as found by Tans et al. (1989). In particular there is a strong sink at mid-latitudes of the northern hemisphere. A

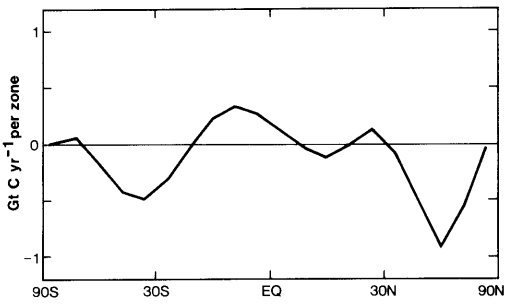

Fig. 5. Non-fossil net surface sources (positive values) and sinks (negative values) of atmospheric carbon in Gt C yr^{-1} per zone of 18×10^{12} m^2, calculated taking the role of CO into account.

similar sink is inferred from three-dimensional modelling studies by Keeling et al. (1990b) and Tans et al. (1990). In our previous study, we suggested that a significant part of this sink must be biotic since the northern hemisphere sink was greater than the southern sink in spite of the smaller ocean area in the north. Tans et al. (1990) have recently presented much stronger evidence in support of this conclusion by showing that the p_{CO_2} difference between the atmosphere and the ocean in the northern hemisphere is too small to account for the amount of ocean uptake predicted on the basis of global carbon cycle models, let alone the larger uptake shown in Fig. 5.

The contour plot of the space-time variation of CO_2 sources differs little from that presented by Enting and Mansbridge (1989, Fig. 7). In our previous work we suggested that the main indication of tropical deforestation is in the strong seasonal cycle in the tropics which we tentatively interpreted as dry-season burning of cleared biomass. In that work we suggested that the omission of CO from the model might account for the failure of the annual mean source to reflect a large CO_2 release. However inclusion of the CO correction has not greatly increased our estimates of the annual mean tropical source in spite of the inclusion of an extra 0.56 Gt C yr^{-1}. This is due to a number of cancellations as shown in Fig. 4. If, as described below, the Tans et al. (1990) results imply that there is a strong biotic sink due to CO_2 fertilisation in the northern hemisphere, then a similar sink is to be expected in the tropics, thereby explaining the failure of this and other modelling studies to reconcile the observed spatial gradients with a

tropical source of the size expected from the combination of oceanic CO_2 release and deforestation.

Our result that, even on a regional basis, the CO contribution to the atmospheric carbon budget is relatively small, results from a number of near cancelations and so we need to check whether this still occurs if our compromise CO budget is modified within the range of current uncertainties. As an extreme case we scale the oxidation sink from 0.86 Gt C yr^{-1} to 1.12 Gt C yr^{-1}. This is based on scaling the sink strength which Fraser et al. (1986) calculated using a mean OH concentration of 7×10^5 radicals cm^{-3} by 9.1/7 to correspond to the upper limit of the OH concentration estimated by Prinn et al. (1987) from analysis of methyl chloroform data. We increase the biotic CO source to 0.82 Gt C yr^{-1} to balance this sink. These changes increase the north-south correction from 0.25 Gt C yr^{-1} to 0.29 Gt C yr^{-1}, but make very little change to the spatial pattern of the correction.

5. The tropical CO_2 budget

We now examine the atmospheric carbon budget for the region 12°S to 12°N in more detail. The annual mean source estimated by our inversion calculation is 0.615 Gt C yr^{-1}. This is expected to be the result of a combination of release from the ocean, release due to deforestation and uptake by extra growth due the fertilising effect of increased CO_2. The magnitude of such a fertilisation effect is hard to predict on physiological grounds. However some such uptake seems to be the only way to account for the fact that the tropical regions do not appear to be a net source of terrestrial CO_2 in spite of the directly observable large-scale deforestation.

In order to quantify the possible releases, we take the estimate of oceanic CO_2 release (0.67 to 1.10 Gt C yr^{-1}) given by Tans et al. (1990) for the region 10°S to 10°N and scale them by 1.2 to apply to our region 12°S to 12°N. Denoting the deforestation release by D and the biotic fertilisation uptake by G, the range of oceanic release quoted by Tans et al., combined with our estimate of the net source, translates into the constraints (assuming a CO oxidation rate of 0.86 Gt C yr^{-1}):

$$-0.633 \leqslant D - G \leqslant -0.117 \qquad (15)$$

For the larger CO oxidation rate of 1.12 Gt C yr^{-1}, the constraints become:

$$-0.705 \leqslant D - G \leqslant -0.189. \qquad (16)$$

Such constraints can be represented graphically by the region lying between the two diagonal lines shown in Fig. 6. (We have plotted case (16) to emphasize the shift away from the origin.) By definition we assume $D \geqslant 0$ and $G \geqslant 0$. A surprising aspect of our analysis is that we find $G > D$, i.e. our net release lies below the range of ocean releases estimated by Tans et al. (1990), implying that the terrestrial biomass in the region 12°S to 12°N is increasing, in spite of the directly observed deforestation.

This type of analysis represents a linear programming approach to the inversion. A general discussion is given by Tarantola (1987) and an example is given by Enting and Mansbridge (1987c). A more refined analysis would work in more than the two dimensions shown in Fig. 6, and include the range of net sources resulting from various values of the CO oxidation and also weaken these constraints slightly to allow for

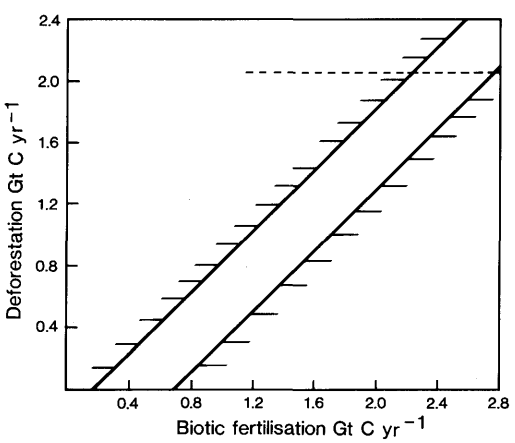

Fig. 6. Possible combinations of annual mean carbon fluxes from deforestation and CO_2-induced growth for the region 12°S to 12°N (assuming the upper limit of the CO oxidation rate). The two diagonal lines bound a region consistent with our estimated annual mean net source and the range of ocean fluxes estimated by Tans et al. (1990). The dashed line is an approximate upper bound calculated on the assumption that all deforestation release is from seasonal biomass burning and that all the seasonal variation in the source is from this process.

uncertainties in the inversion calculation. Our results must be treated with caution because of the limited resolution of the inversion calculation. Clearly a more detailed analysis of the error structure of the inversion is required.

Any further constraints on the possible combinations of fertilisation and deforestation require additional information or assumptions. One possible path forward is to recall the suggestion of Enting and Mansbridge (1989) that the seasonal signal in the tropics was due to biomass burning. If we take the extreme view of attributing *all* of the seasonality in the tropical sources to seasonal biomass burning, then analysis of our source data gives an annual mean release rate of 2.06 Gt C yr^{-1}. (This rate is the sum over zones 9 to 12 of the difference between the annual mean and the annual minimum of our estimated source for each zone.) In reality, the seasonal variations in rainfall that lead to the seasonality in biomass burning will almost certainly lead to seasonal variations (with a phase similar to that of our source estimates) in natural biotic processes. Indeed the fact that our release peaks as much as 2 months earlier than expected for biomass burning (see Enting and Mansbridge, 1989, Fig. 7) may be an indication that other processes are occuring but any attempt to quantify this would require more precision than is justifiable from our inversion calculation. However we feel that we can plausibly argue that $D < 2.06$ Gt C yr^{-1}. This approximate bound is shown by the dashed line in Fig. 6.

If we accept that $D < 2.06$ Gt C yr^{-1} then we can see from Fig. 6 that $G < 2.8$ Gt C yr^{-1}. This is more than the 1 to 2 Gt C yr^{-1} uptake that Tans et al. (1990) suggest for the northern temperate regions when regarded in absolute terms. However, as a proportion of the biomass, the northern hemisphere uptake proposed by Tans et al. is much larger than our approximate upper bound for the tropical uptake. This may reflect real differences between the physiology of CO_2 fertilisation in the two regions. In addition, some of the northern uptake may be due to regrowth of forests on previously cleared land rather than CO_2 fertilisation.

6. Global CO_2 budget

The re-interpretation of the atmospheric carbon budget by Tans et al. (1990) involves three steps.

(i) The distribution of atmospheric CO_2, as interpreted by both forward and inverse modelling studies, indicates a weak southern hemisphere sink and a stronger northern sink (cf. Fig. 5).

(ii) Ocean p_{CO_2} data from northern latitudes indicates that the northern sink is not oceanic and so is presumably biotic.

(iii) If there is a northern biotic sink due to CO_2-induced growth then a similar sink could be expected in tropical regions. This would cancel the source from deforestation and so could explain the inability of modelling studies (Pearman et al., 1983; Pearman and Hyson, 1986; Enting and Mansbridge, 1989, Tans et al., 1989 and the present study) to detect a strong tropical source from the observed spatial gradients of CO_2.

The analysis of the role of the terrestrial biota relies on the fundamental mass-balance equation of the atmosphere:

$$\dot{C}(t) = R(0)[S(t) - \Phi(t)] \tag{17}$$

$$= R(0)[F(t) + B(t) - \Phi(t)]. \tag{18}$$

Here, the response function, $R(t)$, gives the amount of carbon remaining in the atmosphere at a time t after a unit pulse source, $C(t)$ is the atmospheric CO_2 concentration at time t (and the dot denotes differentiation with respect to time), $\Phi(t)$ is the net rate of oceanic CO_2 uptake and $S(t)$ represents the net non-ocean CO_2 source which is assumed to be the sum of a fossil fuel component, $F(t)$ and a biotic component, $B(t)$. In the absence of direct measurements, $\Phi(t)$ must be calculated using some form of carbon cycle model before the mass-balance equation can be used to deduce $B(t)$ from known values of $F(t)$ and observed concentrations, $C(t)$.

It is a general property of such models that the current uptake will depend on the past history of the source (or equivalently of the concentration). If the oceanic uptake processes are constant, and respond linearly to perturbations, then we can follow Oeschger and Heimann (1983) and analyse the problem in terms of response functions, giving the relation

$$Q(t) = C(t) - C(0) = \int_0^t R(t - t')\, S(t')\, dt'. \tag{19}$$

From this relation one can derive (assuming $S(0)=0$):

$$\dot{C}(t) = R(0)\, S(t) + \int_0^t \dot{R}(t-t')\, S(t')\, \mathrm{d}t' \qquad (20)$$

$$= \int_0^t R(t-t')\, \dot{S}(t')\, \mathrm{d}t'. \qquad (21)$$

Relation (20) shows clearly that the connection between current sources and the current rate of increase of CO_2 depends on the past source history. (The relations above are differential forms of the integral relations given by Oeschger and Heimann.) Enting and Mansbridge (1987b) pointed out that there was a generic inversion relation for the convolution (19) as

$$S(t) = \dot{Q}(t)/R(0) - Q(t)\, \dot{R}(0)/R(0)^2 - \int_0^t K(t-t')\, Q(t')\, \mathrm{d}t'. \qquad (22)$$

(The kernel, K, is related to the response function R; the connection is most conveniently expressed in terms of Laplace transforms. In particular, K vanishes if R is a simple exponential.) Eq. (20) shows how a determination of sources at time t requires a knowledge of the concentration at all previous times. For CO_2, Siegenthaler and Oeschger (1987) have performed such deconvolutions using a range of carbon cycle models with data from ice cores. Their numerical technique involved working directly with numerical models, using $C(t)$ as a constraint, rather than determining response functions and using eq. (20). The uncertainties in these inversions, including the question of what information can be obtained from incomplete concentration records, are discussed further by Enting and Newsam (1990b).

Substituting the inversion relation into the equations for the ocean uptake gives:

$$\Phi(t) = -Q(t)\, \dot{R}(0)/R(0)^2 - \int_0^t K(t-t')\, Q(t')\, \mathrm{d}t'. \qquad (23)$$

This has the advantage that the unknown (or at least contentious) source history has been eliminated from the analysis so that questions about ocean uptake are related directly to the concentration history and the model properties. This allows us to focus more directly on which model properties are important than would be the case if we had used a model indirectly to determine $S(t)$.

A number of calculations can be performed to look at ocean models with very small carbon uptake. In particular we consider a mixed layer with a simple first order loss (with time constant τ) into deeper layers. For this model, $R(0) = 0.47$ ppmv Gt^{-1}, $R(0)/\dot{R}(0) = k^{-1}$ the atmospheric turnover time, and

$$K(t) = \frac{k^2\eta}{R(0)} \exp(-(k\eta + 1/\tau)\, t), \qquad (24)$$

where η is the buffer factor $\times$ the pre-industrial ratio of carbon contents in the atmosphere and mixed layer.

In the limit $1/\tau \to 0$, i.e., the atmosphere interacts only with the mixed layer, it turns our that Φ is determined by simply the current rate of increase of CO_2. An increase of 1.5 ppmv yr^{-1} corresponds to $\Phi = 0.3$ Gt C yr^{-1} for $k = 8$ yr. This extreme case emphasises just how large the discrepancy is between the Tans et al. estimates of Φ ($0.5 - 1.0$ Gt C yr^{-1}) and our current understanding of oceanic uptake ($\Phi \approx 2$ Gt C yr^{-1}). The lower end of the Tans et al. range would have the atmospheric CO_2 mixing into an effective ocean volume of less than twice the volume of the mixed layer.

The conventional view of oceanic uptake of CO_2 is based largely on global carbon cycle models calibrated with ^{14}C. Enting (1985) presented a preliminary analysis of this process in terms of response functions, indicating that the calibration could be expected to be ill-conditioned. (A discussion of the ill-conditioning as it relates the calibration of numerical models of the global carbon cycle is given by Enting and Pearman, 1987). Following the work of Tans et al., (1990), Enting (1990) extended the earlier response function analysis and suggested that uncertainties in the biotic uptake of ^{14}C could lead to considerable uncertainties in the calibration of oceanic CO_2 uptake using ^{14}C.

The response function analysis was supplemented by a number of more detailed studies (to be reported elsewhere) using a modified version of the box diffusion model employed by Siegenthaler and Oeschger (1987). These failed to find any combination of physically acceptable model parameters

that could give such low oceanic uptakes, even when the biotic release history was regarded as a completely unknown function to be determined by deconvolution of the atmospheric CO_2 concentration, except in cases in which the terrestrial biota were able to take up large amounts of the ^{14}C from nuclear testing.

In summary, the main possible explanations for the results of Tans et al. (1990) are:

(i) very small vertical mixing in the oceans;
(ii) errors in the measurement, interpretation or extrapolation of p_{CO_2} data; or
(iii) non-stationary behaviour of oceanic mixing, possibly in response to climatic change.

One tentative indication of a possible change in the oceanic uptake can be seen in the fact that the modelling study by Pearman and Hyson (1986) was in agreement with the conventional view of the atmospheric carbon budget and had a strong southern hemisphere ocean sink. While the model had important differences from the model used here (and that of Tans et al., 1989) it would seem that much of the difference in the results may have come from differences in the data that were analysed. We have replotted the annual means that they used (shifted by a constant concentration) as open circles in Fig. 1.

The older data show a much greater change across the southern hemisphere and less across the northern hemisphere. There are however a number of limitations preventing us from unequivocally accepting this difference as evidence of a change in oceanic uptake. There are various intercalibration problems since the older data are a mixture of data from Scripps Institution of Oceanography, NOAA/GMCC and CSIRO. (In the present study, the annual means are based on GMCC data only.) Secondly, it will be seen that there is considerable scatter in the older southern hemisphere data and so the change across the southern hemisphere is subject to some uncertainty. The third point to note in connection with the possible changes in the interhemispheric gradient is that the greatest difference between the two data sets shown is for stations (Ascension Is., Cosmos, Peru, Seycelles, Fanning Is.) for which the earlier data come from quite short records. This is less of a limitation for Samoa.

A number of analyses that seem to contradict such a possibility of reduced gradients in the southern hemisphere and increased gradients in the northern hemisphere are given by Keeling et al. (1990a). In particular, they find that the concentration difference between the South Pole and Mauna Loa increased steadily until about 1975 and then remained relatively constant. This is in line with the pattern of fossil fuel usage as if the fraction of oceanic uptake in the southern hemisphere was in proportion to the releases. The modelling studies presented by Keeling et al. (1990b) find their best fit with a hypothetical strong northern hemisphere oceanic sink for each of the time periods (1962, 1968, 1980, 1984) that they consider. The question of how (or if) such a sink can be reconciled with the p_{CO_2} data used by Tans et al. (1990) remains unresolved.

7. Conclusions

The main conclusion to be drawn from our inversion study is that our calculations confirm that the atmospheric CO_2 data imply a strong northern sink of CO_2 and that the southern hemisphere sink is disproportionately weak. This confirms the results of a number of other modelling studies (Enting and Mansbridge, 1989; Tans et al., 1989; Keeling et al., 1990b, Tans et al., 1990). The correction for the role of CO reduces the degree of this disproportion between uptake and area of ocean but not to the extent expected under the conventional view of the atmospheric carbon budget and it still seems necessary to interpret some of the northern sink as biotic, especially given the p_{CO_2} data presented by Tans et al. (1990).

Thus we are left with two questions: why are the biota taking up so much carbon and why aren't the oceans taking up carbon to the extent indicated by ^{14}C data?

Increased biotic uptake could be accounted for by the fertilising effect of atmospheric CO_2. This would give not only a strong northern sink but also a tropical CO_2 sink that would mask the source due to tropical deforestation. Our results actually suggest that in the region 12°S to 12°N the terrestrial biota are a net sink of carbon but if the oceanic release is near the lower end of the range given by Tans et al. (1990) then the uncertainties in the inversion calculation could admit a weak net carbon source for this region.

With regard to the oceans, the low uptakes

found by Tans et al. (1990) seem at first sight to be too small to be consistent with data on ^{14}C from nuclear testing if the ocean uptake processes are regarded as unchanging. Comparison of the data used in the present study with that analysed by Pearman and Hyson (1986) suggests (subject to many qualifications about comparability of the data) that there has been a significant decrease in the gradient across the southern hemisphere. However the data presented by Keeling et al. (1990a) do not suggest such a change. Alternatively, the analysis by Enting (1990) suggests that if the biotic uptake of ^{14}C from nuclear testing is significantly larger than previously believed, then it may be possible to reconcile the atmospheric ^{14}C record with low (≈ 1 Gt C yr^{-1}) oceanic uptake of CO_2. Clearly further analysis is needed in order to resolve these questions.

An important caveat on these results concerns the limitations of the inversion calculations. The results are sensitive to uncertainties in both the model and data. While Mansbridge and Enting (1989) have studied the sensitivity of source estimates to changes in the model, the lack of quantitative information on the likely size of model errors makes it impossible to translate these sensitivities into error bounds for the source estimates. In addition, Mansbridge and Enting give only limited analyses of the sensitivity to data error. A more complete error analysis is called for.

8. Acknowledgements

The authors acknowledge valuable discussions with R. J. Francey on the significance of our results. We also wish to thank P. P. Tans for supplying a preprint of the Tans et al. (1990) paper and for many stimulating discussions about that work.

REFERENCES

Beardsmore, D. J. and Pearman, G. I. 1987. Atmospheric carbon dioxide measurements in the Australian region: data from surface observatories. *Tellus 39B*, 42–66.

Bolin, B. and Bischof, W. 1970. Variations of the carbon dioxide content of the northern hemisphere. *Tellus 22*, 431–442.

Conway, T. J., Tans, P., Waterman, L. S., Thoning, K. W., Masarie, K. A. and Gammon, R. H. 1988. Atmospheric carbon dioxide measurements in the remote global troposphere, 1981–1984. *Tellus 40B*, 81–115.

Crutzen, P. J. 1987. Role of the tropics in atmospheric chemistry. In: *The geophysiology of Amazonia* (ed. R. E. Dickinson). New York: John Wiley. 107–132.

Crutzen, P. J. and Gidel, L. T. 1983. A two-dimensional photochemical model of the atmosphere. 2: the tropospheric budgets of the anthropogenic chlorocarbons, CO, CH_4, CH_3Cl and the effect of various NO_x sources on tropospheric ozone. *J. Geophys. Res. 88*, 6641–6661.

Enting, I. G. 1985. A classification of some inverse problems in geochemical modelling. *Tellus 37B*, 216–229.

Enting, I. G. 1990. Ambiguities in the calibration of carbon cycle models. *Inverse Problems 6*, L39–L46.

Enting, I. G. and Mansbridge, J. V. 1986. *Description of a two-dimensional atmospheric transport model.* Division of Atmospheric Research Technical Paper No 11. CSIRO Australia.

Enting, I. G. and Mansbridge, J. V. 1987a. *Preliminary studies with a two-dimensional model using transport fields derived from a GCM.* Division of Atmospheric Research Technical Paper No. 14. CSIRO Australia.

Enting, I. G. and Mansbridge, J. V. 1987b. Inversion relations for the deconvolution of CO_2 data from ice cores. *Inverse Problems 3*, L63–L69.

Enting, I. G. and Mansbridge, J. V. 1987c. The incompatability of icecore CO_2 data with reconstructions of biotic CO_2 sources. *Tellus 39B*, 318–325.

Enting, I. G. and Mansbridge, J. V. 1989. Seasonal sources and sinks of atmospheric CO_2: Direct inversion of filtered data. *Tellus 41B*, 111–126.

Enting, I. G. and Newsam, G. N. 1990a. Inverse problems in atmospheric constituent studies: II. Sources in the free atmosphere. *Inverse Problems 6*, 349–362.

Enting, I. G. and Newsam, G. N. 1990b. Atmospheric constituent inversion problems: Implications for baseline monitoring. *J. Atmos. Chem. 11*, 69–87.

Enting, I. G. and Pearman, G. I. 1987. Description of a one-dimensional carbon cycle model calibrated using techniques of constrained inversion. *Tellus 39B*, 459–476.

Francey, R. J., Pearman, G. I. and Beardsmore, D. J. 1988. A southern view of the global atmosphere. *Proc. Roy. Soc. Tas. 122*, 113–119.

Fraser, P. J., Hyson, P., Coram, S., Rasmussen, R. A., Crawford, A. J. and Khalil, M. A. K. 1986. Carbon monoxide in the southern hemisphere. pp341–352 of *Proceedings of the 7th World Clean Air Conference.* (ed. H. H. Hartmann) Clean Air Society of Australia and New Zealand.

Friedli, H., Siegenthaler, U., Rauber, D. and Oeschger, H. 1987. Measurements of concentration, $^{13}C/^{13}C$ and $^{18}O/^{16}O$ ratios of tropospheric carbon dioxide over Switzerland. *Tellus 39B*, 80–88.

Houghton, R. A., Hobbie, J. E., Melillo, J. M., Moore, B., Peterson, B. J., Shaver, G. R. and Woodwell, G. M. 1983. Changes in the carbon content of terrestrial biota and soils between 1860 and 1980: A net release of CO_2 to the atmosphere. *Ecol. Monog. 53*, 235–262.

Keeling, C. D., Whorf, T. P., Heimann, M., and Mook, W. M. 1990a. A three-dimensional model of atmospheric CO_2 transport based on observed winds: 1. Analysis of observational data. *AGU Monograph 55*. Washington, American Geophysical Union. 165–236.

Keeling, C. D., Piper, S. and Heimann, M. 1990b. A three-dimensional model of atmospheric CO_2 transport based on observed winds: 4. Mean annual gradients and interannual variations. *AGU Monograph 55*. Washington, American Geophysical Union. 305–363.

Mansbridge, J. V. and Enting, I. G. 1989. *Sensitivity studies in a two-dimensional atmospheric transport model.* Division of Atmospheric Research Technical Paper, No. 18. CSIRO Australia.

Matthews, E. and Fung, I. Y. 1987. Methane emission from natural wetlands: global distribution, area, and environmental characteristics of sources. *Global Biogeochemical Cycles 1*, 61–86.

Newsam, G. N. and Enting, I. G. 1988. Inverse problems in atmospheric constituent studies: I. Determination of surface sources under a diffusive transport approximation. *Inverse Problems 4*, 1037–1054.

Oeschger, H. and Heimann, M. 1983. Uncertainties of predictions of future atmospheric CO_2 concentrations. *J. Geophys. Res. 88C*, 1258–1262.

Olson, J. S. 1982. Earth's vegetation and atmospheric carbon dioxide. *Carbon Dioxide Review 1982.* (ed. W. C. Clark) Oxford, Clarendon Press.

Pearman, G. I. and Hyson, P. 1986. Global transport and inter-reservoir exchange of carbon dioxide with particular reference to stable isotopic distributions. *J. Atmos. Chem. 4*, 81–124.

Pearman, G. I., Hyson, P. and Fraser, P. J. 1983. The global distribution of atmospheric carbon dioxide: 1. Aspects of observations and modelling. *J. Geophys. Res. 88C*, 3581–3590.

Plumb, R. A. and Mahlman, J. D. 1987. The zonally-averaged transport characteristics of the GFDL general circulation/transport model. *J. Atmos. Si. 44*, 298–327.

Prinn, R., Cunnold, D., Rasmussen, R., Simmonds, P., Alyea, F., Crawford, A., Fraser, P. and Rosen, R. 1987. Atmospheric trends in methyl chloroform and the global average for the hydroxyl radical. *Science 238*, 945–950.

Siegenthaler, U. 1983. Uptake of excess CO_2 by an outcrop-diffusion model of the ocean. *J. Geophys. Res. 88C*, 3599–3608.

Siegenthaler, U. and Oeschger, H. 1987. Biospheric CO_2 emissions during the past 200 years reconstructed by deconvolution of ice core data. *Tellus 39B*, 140–154.

Seiler, W. and Conrad, R. 1987. Contribution of tropical ecosystems to the global budgets of trace gases especially CH_4, H_2, CO and N_2O. In: *The geophysiology of Amazonia* (ed. R. E. Dickinson). New York: John Wiley. 133–162.

Tanaka, M., Nakazawa, T. and Aoki, S. 1987. Time and space variations of tropospheric carbon dioxide over Japan. *Tellus 39B*, 3–12.

Tans, P. P., Conway, T. J. and Nakazawa, T. 1989. Latitudinal distribution of the sources and sinks of atmospheric carbon dioxide derived from surface observations and an atmospheric transport model. *J. Geophys. Res. 94D*, 5151–5172.

Tans, P. P., Fung, I. Y. and Takahashi, T. 1990. Observational constraints on the global atmospheric CO_2 budget. *Science 247*, 1431–1438.

Tarantola, A. 1987. *Inverse problem theory: methods for data fitting and model parameter estimation* (Elsevier, Amsterdam).

Weiss, W., Sittkus, A., Stockburger, H., Sartorius, H. and Münnich, K. O. 1983. Large-scale atmospheric mixing derived from the meridional profile of krypton-85. *J. Geophys. Res. 88C*, 8574–8578.